Infrared Interferometric Measurements of the Near-Surface Air Temperature over the Oceans

P. J. MINNETT, K. A. MAILLET, AND J. A. HANAFIN*

Division of Meteorology and Physical Oceanography, Rosenstiel School of Marine and Atmospheric Science, University of Miami, Miami, Florida

B. J. OSBORNE

Space Science and Engineering Center, University of Wisconsin—Madison, Madison, Wisconsin

(Manuscript received 8 October 2004, in final form 21 December 2004)

ABSTRACT

The radiometric measurement of the marine air temperature using a Fourier transform infrared spectroradiometer is described. The measurements are taken by the Marine-Atmospheric Emitted Radiance Interferometer (M-AERI) that has been deployed on many research ships in a wide range of conditions. This approach is inherently more accurate than conventional techniques and can be used to determine some of the error characteristics of the standard measurements. Examples are given from several cruises ranging from the Arctic to the equatorial Pacific Oceans. It is shown that the diurnal heating signal in radiometric air temperatures in the tropical Pacific can typically reach an amplitude of ~15% of that measured by conventional sensors. Conventional data have long been recognized as being contaminated by direct solar heating and heat island effects of the ships or buoys on which they are mounted, but here this effect is quantified by comparisons with radiometric measurements.

1. Introduction

Measurements of the temperature of the air near the earth's surface have been made for centuries by reading conventional thermometers in enclosures designed to prevent elevation of the measurement by direct heating of the thermometer by sunlight. Over the ocean, where measurements are taken from ships or buoys, the problem of contamination of the air temperature measurement can become much more severe as the presence of a metal structure, a very large structure in the case of some ships, perturbs the marine environment to an unknown degree. Not only does the structure of the ship or buoy disturb the airflow, but also on sunny days, especially in the Tropics, the solar heating of the ship or buoy can elevate the measured air temperature, even if the thermometer is in a screened enclosure (Goerss and Duchon 1980; Ramage 1984; Kent et al. 1993; Berry et al. 2004; Berry and Kent 2005). The result is that even if the thermometer were well calibrated and carefully maintained, so that it were to give an accurate measurement, that measurement may not be of what is required. What is needed is a determination of the air temperature that would be made if the ship or buoy were not there. This paradox can be resolved by using a radiometer to measure the air temperature, in which case the thermal emission of molecules in the air is collected, and with the correct selection of the infrared spectral intervals and an appropriate geometry of the instrument, a determination of the air temperature away from the perturbing effects of the ship or buoy can be made. This approach was adopted by Shaw et al. (2001), who used a simple filter radiometer with a rotating scan mirror to sweep the field of view in a vertical plane. When the radiometer viewed downward, a skin SST was taken, and when the radiometer viewed the upper segment of the scan, an air temperature measurement was made. One of the difficulties of this simple

* Current affiliation: Space and Atmospheric Physics, Imperial College, London, United Kingdom.

Corresponding author address: Dr. P. J. Minnett, Division of Meteorology and Physical Oceanography, Rosenstiel School of Marine and Atmospheric Science, University of Miami, 4600 Rickenbacker Causeway, Miami, FL 33149.
E-mail: pminnett@rsmas.miami.edu

and elegant technique is providing good calibration data during the scan. A further problem is the selection of an appropriate spectral interval for the measurement.

This paper presents an alternative approach to measuring the air temperature using a well-calibrated Fourier transform infrared (FTIR) spectroradiometer, the Marine-Atmospheric Emitted Radiance Interferometer (M-AERI; Minnett et al. 2001). The next section of this paper presents a brief discussion of the accuracies required of measurements of the marine air temperature. Then M-AERI is summarized and the selection of the optimized infrared spectral intervals is discussed. Examples of air temperatures measured by M-AERI taken from several cruises are presented, and the closing discussion presents some of the advantages this approach offers over conventional air temperature measurement techniques used at sea.

The validation of the M-AERI radiometric measurements of air temperatures is problematic in that it inevitably involves comparisons with conventional measurements, which are believed to be inaccurate in certain circumstances. Emphasis is given, therefore, to comparisons at night and under high winds when, it is hoped, the conventional measurements are likely to be correct. The discrepancies between the two types of measurements are then an indication of the corruption of the conventional measurements by extraneous effects, although, as will be shown, there are conditions when the radiometric measurements are themselves susceptible to contamination. Our confidence in the absolute accuracy of the M-AERI measurements is based not only on laboratory measurements but also on comparisons in the field with independently calibrated precision radiometers.

2. Accuracy requirements

The conventionally quoted required accuracy of a marine air temperature measurement is ±0.1 K (e.g., HMSO 1994). This is a compromise between what can be readily obtained in the field, and what would ideally be desired. Clearly, for many applications, the more accurate the measurement can be made, the better. In terms of weather forecasting, the 0.1-K target is a reasonable objective, but in terms of climate research, in which the identification of long-term trends of the size of ~0.1 K decade^{-1} is being sought, a more accurate measurement, or time series of more accurate measurements, would permit the identification of trends to be made sooner and with more confidence.

Another application of the marine air temperatures is in the calculation of air–sea fluxes of heat, momentum, and gases. The sign of the air–sea temperature difference largely determines whether the overlying boundary layer is stable, neutrally stable, or unstable. In stable situations the exchanges, which are facilitated by turbulence in the lower atmosphere, are much smaller than in neutral or unstable situations. In an unstable atmospheric boundary layer, convection resulting from heat flow from a warm sea surface to a cooler overlying atmosphere greatly enhances the vertical transport of heat, momentum, and gases. Given that the air–sea temperature difference over much of the world's oceans is only a degree or so, an uncertainty of a few tenths of a degree in the measurement of either the air or sea surface temperature can lead to a significant error in the calculation of the sensible and latent heat fluxes. Indeed, it is possible that erroneous measurements of the marine air temperatures can lead to errors not only in the magnitude of the air–sea turbulent exchanges, but also in the sign of the fluxes (Minnett 2004). Thus, more accurate measurements of the marine air temperatures can lead to improvements in our understanding of the coupling of the ocean and atmosphere.

3. The M-AERI

The M-AERI is a Fourier transform infrared interferometer that has been adapted to operate for long durations on the deck of a ship at sea while maintaining a high level of absolute accuracy (Minnett et al. 2001). It operates in the range of infrared wavelengths from ~3 to ~18 μm and measures spectra with a resolution of ~0.5 cm^{-1}. It uses two infrared detectors to achieve this wide spectral range, and these are cooled to ~77 K (i.e., close to the boiling point of liquid nitrogen) by a Stirling cycle mechanical cooler to reduce the noise equivalent temperature difference (NEΔT) to levels well below 0.1 K at typical environmental temperatures. The M-AERI includes two internal blackbody cavities for accurate real-time calibration. A scene mirror directs the field of view from the interferometer to either of the blackbody calibration targets or to the environment from nadir to zenith. The mirror is programmed to step through a preselected range of angles. The control computer integrates measurements over a preselected time interval, usually a few tens of seconds, to obtain a satisfactory signal-to-noise ratio (SNR). A typical cycle of measurements including two view angles to the atmosphere, one to the ocean, and calibration measurements, takes about 5–10 min, depending on the number of independent interferograms averaged to produce each spectrum. The M-AERI is equipped with pitch and roll sensors so that the influ-

ence of the ship's motion on the measurements can be determined.

The radiometric calibration of the M-AERI is done continuously throughout its use in the field; as with simpler self-calibrating radiometers, an FTIR spectroradiometer can be calibrated by using two blackbody targets at known temperatures. These provide two reference spectra to determine the gains and offsets of the detectors and associated electronics. Since the instrument measures interferograms rather than spectra or spectrally integrated radiance (as is the case with a bandpass filter radiometer), it is important that the calibration be independent of the positions of the moving mirrors. This is achieved by very careful design and assembly, so that the effective aperture size, and its projection onto the detectors, is insensitive to pathlength differences (Revercomb et al. 1988). The mirror scan sequence includes measurements of the reference cavities before and after each set of spectra from the ocean and atmosphere. The absolute accuracy of the infrared spectra produced by the M-AERI is determined by the effectiveness of the blackbody cavities as calibration targets. Each blackbody cavity is a copper cylinder with conical end plates, one with a circular orifice to allow the radiation to emerge. The internal walls are painted matte black and the cavity has an effective emissivity of >0.998. During construction the blackbody thermistors are calibrated against thermometers traceable to National Institute of Standards and Technology (NIST) standards.

The SNR is a function of position in the spectrum and the temperature of the target scene. The noise equivalent radiance (NEΔL) for the cooled HgCdTe detector is <0.2 mW $(\text{m}^2\ \text{sr}\ \text{cm}^{-1})^{-1}$, and for typical terrestrial temperatures, the atmospheric emission is $\sim$160 mW $(\text{m}^2\ \text{sr}\ \text{cm}^{-1})^{-1}$ at $\sim$670 cm^{-1} ($\lambda = 15\ \mu$m), giving an SNR of >800 for a single measurement (Minnett et al. 2001).

An independent determination of the absolute radiometric accuracy was made during two infrared radiometry workshops held at the University of Miami in early 1998 (Kannenberg 1998) and 2001 (Rice et al. 2004; Barton et al. 2004). The internal calibration of the M-AERI is checked periodically using a water-bath blackbody calibration target (Fowler 1995). The M-AERI is mounted so the axis of the scan mirror is at the same height as, and orthogonal to, the axis of the blackbody cone. The results of the measurements in a transmissive part of the spectrum are shown in Table 1. The accuracy of the water-bath blackbody calibration target has been assessed by using the NIST Transfer Radiometer (TXR; Rice and Johnson 1998) and was found to be about $\pm$30 mK (Rice et al. 2004). Further details of the M-AERI and its operation are given elsewhere (Minnett et al. 2001).

TABLE 1. Laboratory tests of M-AERI accuracy. The mean discrepancies in the M-AERI measurements of the NIST water bath blackbody calibration target in a transparent spectral interval (wavelengths: 980–985 cm^{-1}) where the atmosphere absorption and emission are low. Discrepancies are M-AERI minus NIST temperatures. (After Minnett et al. 2001; see also Fig. 9, ibid.)

Target temperature	Temperature discrepancy
20°C	+0.013 K
30°C	−0.024 K

4. Spectral selection

There are four major considerations for the selection of appropriate spectral intervals (channels) for the radiometric measurement of air temperature: (i) the channels must have sufficiently low transmissivity to provide a signal of the near-instrument generated atmospheric radiance without a great deal of contribution from farther aloft, for upward-looking measurements, or from the underlying surface for downward-looking measurements; (ii) the channels must, however, be sufficiently transmissive to allow the detectors of the M-AERI to receive the radiation emitted by the reference blackbodies, required for accurate radiometric calibration at those wavenumbers without significant contributions from the, albeit short, atmospheric path; (iii) the channels should be relatively insensitive to variations in atmospheric water vapor, thereby avoiding unwanted correlation errors between the air temperature measurement and humidity fluctuations; and finally, (iv) it is advantageous to identify several channels with similar transmittance so that the instrument noise can be reduced further by averaging the independent measurements.

The spectral region for the measurement of air temperature was chosen to be between 650 and 700 cm^{-1} (wavelengths of 14.28–15.38 μm) where the atmospheric emission is dominated by that from CO_2, a sufficiently well-mixed gas in the lower atmosphere with only a small natural, largely seasonal, variability that contributes little to the uncertainties of the air temperature measurements. Channel selection was performed using a synthetic marine atmosphere of uniform 30°C temperature and 85% humidity as input to the radiative transfer code LBLRTM (see Clough and Iacono 1995, and references therein) with transmittance calculated for a 3-m path. The sensitivity to water vapor of channels within the 650–700 cm^{-1} region of interest was tested by repeating the LBLRTM run with a dry atmo-

sphere; those channels which showed a transmittance change of over 10% were deemed unsuitable. A choice of 16 channels was made to reduce instrumental noise, increasing the SNR to 3200. Note that channels within the same ensemble need not be adjacent in wavenumber space. Three sets of channels were selected, each ensemble having a different average transmittance. For simplicity, the three spectral channel groups are identified by the names "Near-16," "Mid-16," and "Far-16," in order of increasing transmittance (Fig. 1).

Sensing distance

Because of the exponential relationship between transmittance and distance, the sensing properties of the channels are best described through the calculation of weighting functions as shown in Fig. 2. These are for down-looking measurements with an M-AERI altitude of 19 m. The temperature profile varies linearly from 25°C at the surface to 24.81°C at 19 m (i.e., an approximate lapse rate of 1 K (100 m)$^{-1}$. This is slightly greater than the 0.65 K (100 m)$^{-1}$ often used as typical lapse rates in the lower boundary layer; see, e.g., Morris et al. 1973). The relative humidity is set constant for all layers at 85%.

LBLRTM simulations were run 20 times, each time changing the "end-of-path" altitude in 1-m intervals from 18 m to the surface, thus determining the change of transmittance versus height. Figure 2 shows the weighting functions for the three ensembles at three different zenith angles. The ensembles with greater transparency show lesser curvature.

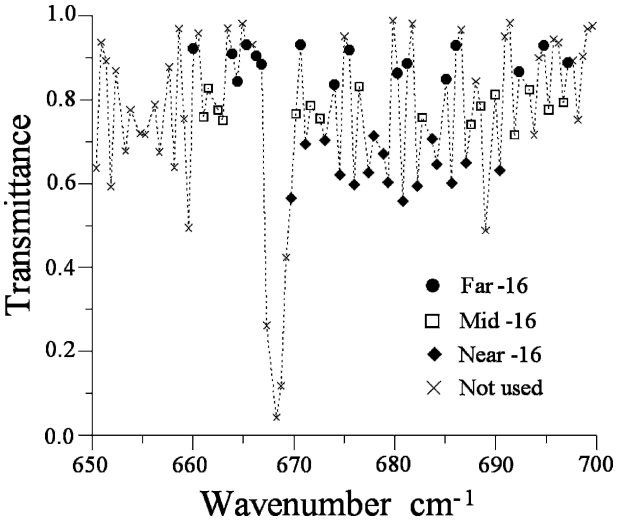

FIG. 1. Transmittance over a 3-m path for wavenumbers in the 650–700 cm^{-1} region, showing channels selected for the Near-, Mid-, and Far-16 channel sounding ensembles. Wavenumbers on this graph are at M-AERI resolution (~0.5 cm^{-1}).

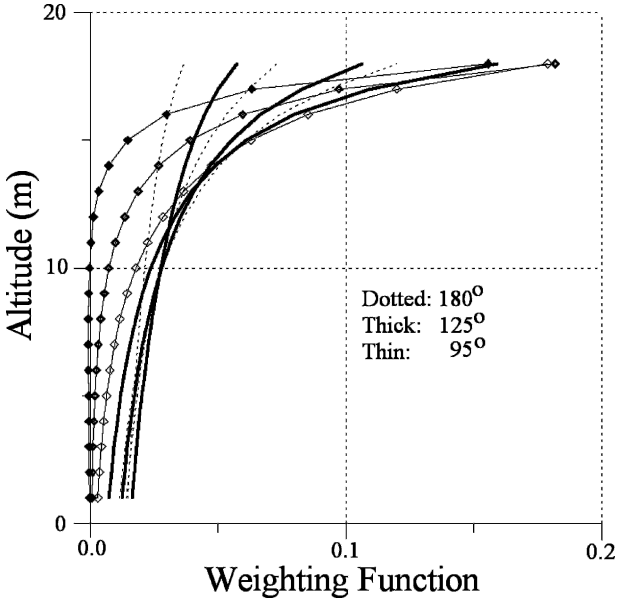

FIG. 2. Weighting functions for the three channel ensembles at three viewing angles (95°, 125°, and 180° from zenith) for a M-AERI mounted at 19 m above sea level. Within each set for each angle, the Near-16 spectral ensemble shows the greatest curvature, and the Far-16 the least.

An alternative method of describing the sensing properties of the three channel ensembles is to indicate at what distance the transmittance is reduced by the factors 1/*e* (~37%), 10%, and 1% for a given wavenumber. For measurements at 669.702 cm^{-1}, for example, LBLRTM calculated a transmittance of τ = 0.5654 for a 3-m path. The *e*-folding length occurs at 5.26 m. This means that, assuming constant temperature over the path, 63% of the M-AERI-received radiance emanates from between the instrument and a distance of 5.26 m. By 24.23 m, only 1% of the received signal comes from a greater distance. Table 2 shows the transmittance information for each of the 16 channels (displayed to two decimal places only for clarity). The average sensing ranges for the Near-16 channel composite, for example, are 6.8, 15.6, and 31.3 m for the *e*-folding length, 10% and 1% point, respectively. The characteristics of the Mid-16 and Far-16 ensembles are given in Table 3.

5. At-sea measurements

The main purpose of the M-AERI deployments at sea is to measure the skin temperature of the ocean. This is the temperature of the submillimeter layer at the ocean surface, and is generally a few tenths of a degree cooler than the water just below (Woodcock and Stommel 1947; Saunders 1967; Katsaros et al. 1977; Donlon

TABLE 2. Transmission properties of the selected air temperature measurement channels. A list of the 16 selected spectral channels used in the air temperature estimate and their transmission properties for typical tropical conditions. The "average range" row shows, e.g., that 90% of the radiance (corresponding to 10% transmittance) received at the M-AERI originates from distances 15.63 m and less, and 99% (1% transmittance) from distances of 31.27 m or less.

Wavenumber (cm^{-1})	Transmittance	k (m^{-1})	e-folding length (m)	10% length (m)	1% length (m)
669.70	0.57	0.19	5.26	12.11	24.23
671.15	0.69	0.12	8.21	18.90	37.80
673.08	0.70	0.12	8.53	19.64	39.29
674.52	0.62	0.16	6.29	14.48	28.96
675.97	0.60	0.17	5.83	13.44	26.87
677.42	0.63	0.16	6.41	14.75	29.51
677.90	0.71	0.11	8.88	20.45	40.89
678.86	0.67	0.13	7.53	17.34	34.67
679.35	0.60	0.17	5.92	13.64	27.28
680.79	0.56	0.19	5.16	11.88	23.76
682.24	0.59	0.17	5.77	13.29	26.58
683.68	0.71	0.12	8.62	19.84	39.67
684.17	0.65	0.15	6.85	15.76	31.53
685.61	0.60	0.17	5.91	13.61	27.21
687.06	0.65	0.14	6.94	15.98	31.96
690.43	0.63	0.15	6.52	15.02	30.04
Average range (m)			6.79	15.63	31.27
Std dev (m)			1.22	2.81	5.61

and Robinson 1996; Minnett 2003). The M-AERI skin temperatures have been made for the validation of surface temperatures derived from the measurements of radiometers on satellites (Kearns et al. 2000; Minnett et al. 2002, 2003; Minnett 2002; Donlon et al. 2002). This objective strongly influences the position on the ships where the M-AERI is installed, and also the sequence of scan mirror angles. The M-AERI is mounted so that it can have a clear view of the sea surface unperturbed by the bow wave of the ships; this is generally achieved with a nadir angle of 55°. To further improve the signal-to-noise ratio, several independent spectral scans are

TABLE 3. Transmission properties of other candidate air temperature measurement channels. Properties of the two additional sets of 16 channels that were candidates for air temperature measurements. The e-folding distances of 11.9 and 28.9 m for the Mid-16 and Far-16 ensembles, respectively, contrast with that of 6.8 m for the Near-16 ensemble (Table 2). Note also the larger spread in sensing distances for the Far-16 case. The standard deviation of Near-16 ensemble e-folding distances is 1.22 m.

Mid-16 ensemble				Far-16 ensemble			
Wavenumber (cm^{-1})	Transmittance	k (m^{-1})	e-folding length (m)	Wavenumber (cm^{-1})	Transmittance	k (m^{-1})	e-folding length (m)
661.02	0.76	0.09	10.86	660.06	0.92	0.03	36.32
661.51	0.83	0.06	15.78	663.92	0.91	0.03	31.27
662.47	0.78	0.08	11.79	664.40	0.84	0.06	17.53
662.95	0.75	0.10	10.46	665.36	0.93	0.02	41.08
670.18	0.77	0.09	11.24	666.33	0.90	0.03	29.56
671.63	0.79	0.08	12.43	666.81	0.88	0.04	24.16
672.60	0.75	0.09	10.67	670.67	0.93	0.02	41.12
676.45	0.83	0.06	16.22	674.04	0.84	0.06	16.66
682.72	0.76	0.09	10.80	675.49	0.92	0.03	35.19
687.54	0.74	0.10	10.00	680.31	0.86	0.05	20.27
688.51	0.78	0.08	12.39	681.27	0.89	0.04	24.75
689.95	0.81	0.07	14.42	685.13	0.85	0.06	18.10
691.88	0.72	0.11	8.98	686.10	0.93	0.02	40.25
693.33	0.82	0.06	15.45	692.36	0.87	0.05	20.72
695.26	0.78	0.08	11.85	694.77	0.93	0.02	40.22
696.70	0.79	0.08	12.95	697.18	0.89	0.04	25.17
Average range (m)			11.85	Average range (m)			28.90
Std dev (m)			2.17	Std dev (m)			9.11

averaged for each skin temperature measurement. Typical M-AERI deployments average over 46 spectra for each of the sea and sky views.

To correct for the reflected sky radiance in the sea-viewing measurement, which is an important part of the derivation of the skin temperature from the M-AERI data, a corresponding measurement of the downwelling emission from the atmosphere is made (Smith et al. 1996; Minnett et al. 2001). This is done at the same zenith angle as the nadir angle of the sea-viewing measurement. Thus each sequence of M-AERI measurements includes spectral data taken at 55° from zenith and nadir.

Ideally, the air temperature measurement would be made from spectra taken with a horizontal view, but the selection of the Near-16 spectral ensemble means that the air temperature can be derived from the slant angle data using a simple arithmetic average. This spares the time in each measurement sequence, and since the usual operation of the M-AERI does not include a horizontal view, air temperature is routinely retrieved as the mean of the air temperature derived at the sky55 and sea55 views. The consequences of this approach were quantified using a series of measurements in which a horizontal view was included in the mirror sequence. The M-AERI was programmed with four view angles: a zenith view angle (zenith), a view angle of 55° from zenith (sky55), a horizontal view angle of 90° from zenith (sky90), and a view angle of 55° from nadir (sea55). With this configuration, we can compare the radiometric air temperatures calculated from the spectra measured at each angle. This experiment was run over many months using the M-AERI installed on the Royal Caribbean Cruise liner *Explorer of the Seas*, which is equipped with oceanographic and atmospheric laboratories (Williams et al. 2002). For the period used here, the *Explorer of the Seas* left Miami each Saturday afternoon and returned the following Saturday morning, following two circuits through the eastern and western Caribbean on alternate weeks. The M-AERI, installed at a height of ~28 m above the waterline, operated continuously throughout, but data from periods in port where dockside structures may interfere with the measurements have been discarded.

Typical variations of the radiance measured in the horizontal view in the spectral interval containing the Near-16 spectral ensemble are plotted in Fig. 3 with the Planck radiance at the retrieved air temperature (300.825 K); also shown are the Planck radiances for a range of temperatures up to ±0.2 K. These data were taken from a single spectrum measured on 29 July 2001. The variation in radiance and brightness temperature in this spectral interval at the different view angles is shown in Fig. 4. As expected, the radiance measured from the horizontal (sky90) view angle falls between that measured from the sky55 and the sea55 view angles. The measured radiance increases from zenith to the sea55 view angle, consistent with an increase in temperature with decreasing altitude, that is, a negative lapse rate.

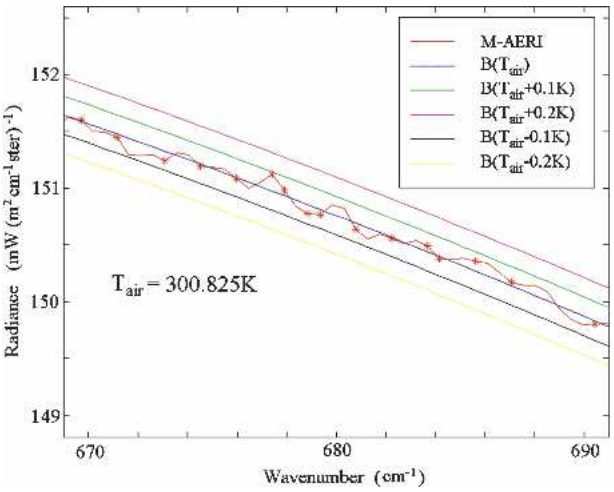

FIG. 3. Typical spectral behavior of radiance measured in the horizontal view angle for the spectral interval used for the air temperature measurement. The red line shows the measured radiances and the stars those points in the Near-16 ensemble. The blue line is the Planck radiance at the retrieved air temperature, and the other colors the Planck radiance for temperatures ±0.1 and ±0.2 K.

The upper panel of Fig. 5 shows the horizontal-view air temperature for a 12-day period at the beginning of 2002. This is an extreme example as it includes the passage of a cold front on day 4 (4 January 2002, UTC) which caused a drop in air temperature of about 12 K in 12 h. This resulted in air–sea temperature differences of over 10 K during this period—a very rare occurrence. The two other marked drops in air temperature are the result of land breezes bringing air that has cooled over the Florida peninsula out over the ship as it approaches Miami during the Friday nights and the following mornings when the ship is in port (days 5 and 12). The second half of this period is much more characteristic of the normal winter conditions along the ship's track. The lower panel shows the differences referenced to the horizontal view (sky90) air temperature measurement of the air temperatures measured at the sea55 (green), sky55 (red), and the average of these (blue). The gaps in the record are when the ship is in port. For all except the most extreme situations, the air temperature computed as the average of the two slant-path measurements agrees with the horizontal measurement to much better than 0.1 K (Table 4). This is true also for typical

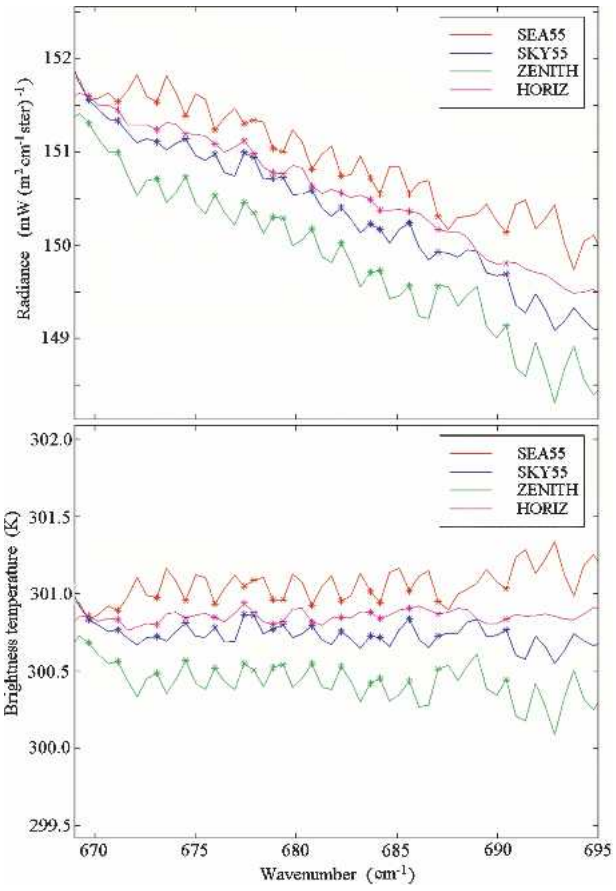

FIG. 4. Examples of (top) measured radiances and (bottom) the equivalent brightness temperatures as functions of wavenumber. The colors denote view angles and the stars mark the wavenumbers used in the air temperature retrievals (Near-16 spectral ensemble).

summer conditions (Table 4). In the period following the passage of the cold front the discrepancies are greater, but still within 0.5 K (mean + standard deviation). The mean differences in the up- and down-looking temperatures referenced to those derived from the horizontal view are in accordance with a curved lapse rate, with greater vertical gradients below the sensor than above. These extreme air–sea temperature differences are very rare occurrences.

a. Comparison with conventional measurements

To establish confidence in the M-AERI air temperature measurements requires comparison with independent measurements though a wide range of conditions and measurement geometries. This has been achieved during a series of research cruises, in which air temperatures were measured using conventional instruments, both of research grade and those used for routine measurements taken according to WMO protocols.

An initial validation of the M-AERI air temperature measurements has already been reported by Minnett et al. (2001), who present a comparison between M-AERI air temperature and those measured by a thermometer on a foremast sensor suite on the NOAA ship *Discoverer*, during the Combined Sensor Cruise in the equatorial and tropical Pacific Ocean in 1996 (Post et al. 1997). They found a mean difference of 0.1 K (M-AERI warm) and a standard deviation of 0.22 K, which include uncertainties in the conventional measurements. These were research-grade air temperature measurements, taken from a purpose-built meteorological mast on the foredeck of the ship. The thermometer was mounted at about the same height as the M-AERI. This comparison was the first step in substantiating our expectation to be able to measure accurately the air temperatures radiometrically.

Subsequent M-AERI deployments on several research cruises where the conventional air temperatures were measured by sensors for routine weather reporting, rather than research, revealed some discrepancies with a strong diurnal nature. A cruise on the Japanese R/V *Mirai* in the tropical Pacific Ocean as part of the United States–Japanese Nauru99 Project from 6 June to 7 July 1999 provided a comparison in very demanding conditions. For most of this time the ship was close to the equator where insolation was high and winds were moderate or low. An M-AERI was installed on a foremast instrument platform at a height of about 14 m above the waterline, and the routine air temperature measurements, recorded as 2-min averages of 2-s samples, were made using a thermometer mounted in a Stevenson's screen behind the wheelhouse. The two sensors were at about the same height. The time series of the measurements are shown in Fig. 6. The conventional measurements possess a large diurnal signal. The corresponding signal is much reduced in the radiometric data. The diurnal characteristics of these discrepancies are shown in Fig. 7a, and can be in excess of 2 K in the middle of the afternoon. They show a repeatable diurnal pattern that is consistent with heating of the conventional sensor by sunlight each day. During this period the daily peak insolation usually exceeded 850 W m^{-2} and the relative winds were 7.5 ± 3.8 m s^{-1} for the whole cruise, although there were periods when the ship was close to the equator where the relative winds were <5 m s^{-1}. The means and standard deviations of the air temperatures measured conventionally were 28.06° ± 0.82°C and measured radiometrically were 27.85° ± 0.37°C for the periods where both data streams were producing data that passed quality assurance tests (see the discussion below). There is a small bias in the air temperature differences measured at

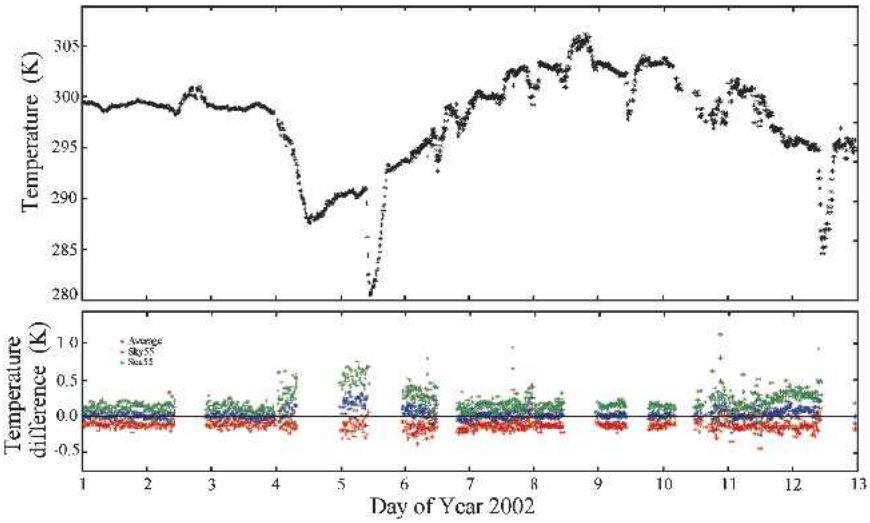

FIG. 5. Time series from the first 12 days of Jan 2002 of air temperature derived from the horizontal view (sky90) of the M-AERI mounted on (top) *Explorer of the Seas*. The cooling signals at days 5.5 and 12.5 are associated with the ship being in the Port of Miami, and on day 4 with the passage of a cold front. The lower panel shows the differences in air temperatures between the horizontal (sky90) measurements and those derived from the upward view (sky55) in red, and the downward view (sea55) in green, and their average in blue. The gaps result from when the ship was in port and the sea55 measurements may have been contaminated by the dockside structures.

night, which reveals what is probably a small calibration uncertainty in the conventional air temperature thermometer.

Figure 7b shows comparable measurements taken from the R/V *Tangaroa* to the southeast of New Zealand from 20 March to 14 April 2004. In this case the conventional measurements were taken from a thermometer as part of a metrological cluster on the mainmast of the ship, and the M-AERI was mounted 10 m above the waterline just ahead of the bridge. Most of the measurements were taken at latitudes about 47°S where wind speeds were high (averaging 12.6 ± 5.4 m s^{-1}) and daily peak insolation, while sometimes reaching 800 W m^{-2}, was generally much less (sometimes <500 W m^{-2}). On some days low winds coincided with clear skies and it was under these conditions that the deviations between the conventional and radiometrically measured air temperatures were greatest. For high winds, when the conventional thermometer was well aspirated, the deviations were muted (Fig. 7b).

b. Low-elevation shipboard deployment

The position of the M-AERI on most ships is sufficiently high that the pathlength to the sea surface in the sea-viewing data is much longer than the 10% length of the Near-16 spectral ensemble used for air temperature measurements. On some ships, however, the arrangement of decks and other equipment dictates that the M-AERI be mounted on the foredeck to ensure the intersection of the M-AERI field of view and the sea surface is ahead of the bow wave. Mounting the M-AERI low and forward on the ship is an acceptable

TABLE 4. Statistics of the air temperature differences. (All values are in K.) The differences are measured at the up-looking and down-looking angles (55° to the vertical), and the averages of these, referenced to the temperature measured in the horizontal view for summer and winter conditions in the Caribbean area. All cases exclude data within 3 n mi of a port. The winter conditions, including the anomalous winter week, are shown in Fig. 5.

View difference	Avg, horizontal	Up, horizontal	Down, horizontal
Summer conditions (29 Jul 2001–4 Aug 2001)			
Mean	0.0086	−0.1153	0.1325
Std dev	0.0901	0.0786	0.1188
Winter conditions (6 Jan 2002–12 Jan 2002)			
Mean	0.0359	−0.1299	0.2017
Std dev	0.0890	0.0744	0.1250
Anomalous winter week (1–5 Jan 2002)			
Prefrontal			
Mean	0.0052	−0.1092	0.1196
Std dev	0.0398	0.0462	0.0560
Postfrontal			
Mean	0.2148	−0.1079	0.5377
Std dev	0.2149	0.2011	0.2876

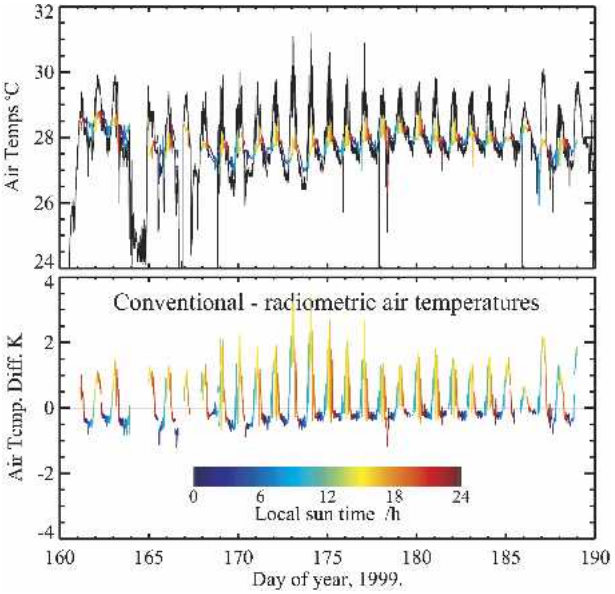

FIG. 6. Time series of air temperature measured on the R/V *Mirai* during the Nauru99 project. (top) The conventional measurements, in black, revealing a very large diurnal signal, and in color the radiometric measurement taken by the M-AERI. The colors represent the local sun time according to the key in the lower panel. The amplitude of the diurnal signal in the radiometric measurements is much smaller. (bottom) The difference between the conventional and radiometric air temperatures. Most of the measurements are taken close to the equator in the western Pacific Ocean. Measurements taken with winds from the starboard stern sector have been removed (see text). Day 160 is 9 Jun, and 190 is 9 Jul. Day numbers on the time axis are UTC.

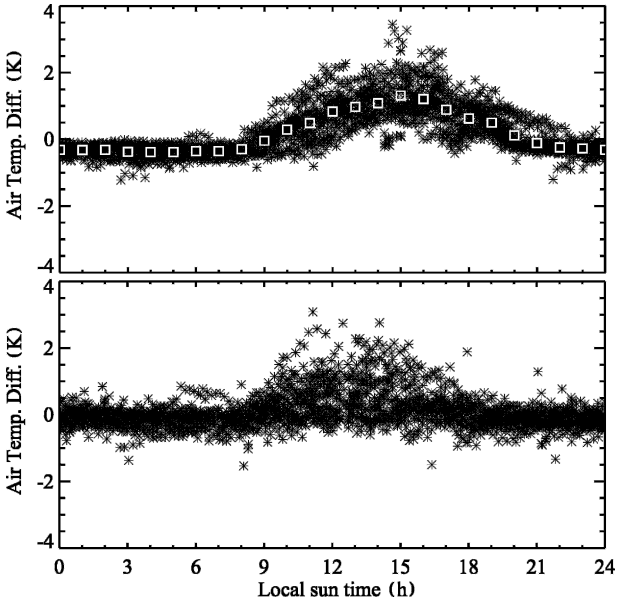

FIG. 7. Discrepancies between conventional measurements of air temperature and radiometric temperatures measured by the M-AERI on (top) R/V *Mirai* and (bottom) R/V *Tangaroa*. The *Mirai* data taken in summer 1999 were in a high insolation, low-to-moderate wind speed regime in the equatorial western Pacific, and the *Tangaroa* measurements were made in Mar and Apr 2004 in the Southern Ocean off New Zealand in predominantly high wind and variable insolation conditions. The *Mirai* data have measurements taken with winds from the starboard stern sector removed (see text), and the white squares are the average values for each hour.

solution if conditions are moderately calm and waves are not expected to break over the bow. This is the situation for M-AERI deployments on the NGCC *Pierre Radisson*, a Canadian Coast Guard icebreaker that has been used for several research programs in the Arctic Ocean. The height of the M-AERI when mounted on the foredeck of the *Radisson* is 6.5 m above the waterline. With a view angle of 55° from nadir, the pathlength to the sea surface is 11.3 m, which means about 19% of the signal in the sea-viewing data of the Near-16 spectral ensemble comes from the surface and not the air. This is expected to lead to a marked dependency of the retrieved air temperature on the air–sea temperature difference.

During a cruise of the *Radisson* in the Northwest Passage and the southeastern Beaufort Sea as part of the Canadian Arctic Shelf Exchange Study (CASES; Fortier 2003) in September and October 2002, the M-AERI was mounted on the foredeck, as was a meteorological tower belonging to researchers from the University of Manitoba. This allowed a comparison between the M-AERI air temperatures and conventional measurements in low-temperature conditions. Comparisons between the M-AERI air temperatures and the measurements of a fine-wire fast-response thermocouple, mounted at a height of 8.6 m above the waterline, and about 10 m ahead of the M-AERI are shown in Fig. 8. The data are presented as discrepancies between the M-AERI (radiometric) and mast (conventional) measurements as a function of the air-to-surface temperature difference as measured by the M-AERI. The stars show the M-AERI data with air temperatures retrieved without taking into consideration the effects of contamination of the sea-viewing data by the surface emission. As expected, there is a strong dependency on the air-surface temperature difference, indicating contamination of the M-AERI air temperature retrievals by surface emission. By assuming a simple linear lapse rate in the lower atmospheric boundary layer, over a height range of a few tens of meters, the effects of the surface emission can be corrected. The plus signs in Fig. 8 show the corrected data. There remains a slight dependency on the air-surface temperature difference, as would be expected given the small height difference between the two sensors, but the major effects of the

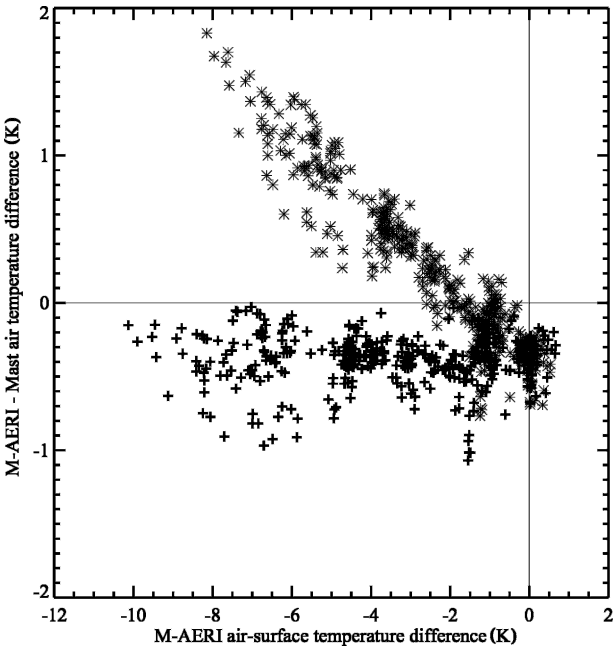

FIG. 8. Discrepancies between the M-AERI radiometric air temperatures and those measured by a thermometer on the meteorological mast on the NGCC *Pierre Radisson*, plotted as a function of the air-surface temperature difference derived from M-AERI measurements. The plus signs indicate the M-AERI air temperature discrepancies after correction for surface radiance contamination, and the stars show data before the correction.

contamination have been removed. The offset between the two records probably reveals a calibration uncertainty in the thermometer on the mast, as this has been designed for fast response to measure turbulent fluctuations and not necessarily for good absolute accuracy. The mean discrepancy is also in the correct sense to be caused by the difference in heights of the two instruments, but if this were the case, the discrepancies would vanish for zero air-surface temperature difference.

6. Discussion

A concern about selecting a set of spectral channels with short atmospheric pathlengths was that the detector might not receive radiances from the internal calibration targets sufficiently uncontaminated by atmospheric emission from the path between the black bodies and the detectors. This concern appears to be unfounded. The sensitivity of the calibration procedure to this effect is much reduced as one of the blackbody cavity calibration targets "floats" at the ambient air temperature, so the effects of the pathlength absorption and emission during this part of the calibration cycle are very small. There may indeed be a small error in the gains of the detector calculated using the hot blackbody target (at 60°C) and the ambient temperature target, as the effect of the intervening atmosphere will be to reduce the radiance received from the warm target at these wavenumbers. This effect is only a few percent at most. However, since the air temperature being retrieved from the spectra is very close to that of the ambient-temperature calibration target, the error in gain introduces a negligible error in the derived air temperature.

Comparisons between radiometric measurements of air temperatures derived from the M-AERI spectra and those measured using conventional thermometers generally show good agreement, at the level of a few tenths of a degree. Perfect agreement would not be expected because of natural variability in the air temperature field. Large discrepancies occur during conditions of low winds speed and high insolation where the conventional measurements are contaminated by additional heating, either directly by the sunshine, or indirectly through heat island effects of the ship. In such cases differences of several degrees can occur. The contamination of routine measurements of air temperature in such conditions has long been recognized (e.g., Goerss and Duchon 1980; Ramage 1984), and is expected also in measurements from much smaller platforms than ships, such as surface moorings (Anderson and Baumgartner 1998). Correction schemes for such measurements have been proposed (e.g., Kent et al. 1993), but without independent data, such as from the M-AERI, it is difficult to know when the corrections have been applied effectively. Many analyses used for climate research are limited to nighttime measurements to avoid diurnal heating effects (Rayner et al. 2003). The insensitivity of the radiometrically determined air temperature to local heat island effects is a great advantage, and it is due to the fact that the measurement is of air that is somewhat removed from the direct influence of the ship. This also renders the measurement less sensitive to flow blockage effects of the ship (e.g., Yelland et al. 1998) that can introduce errors into the conventional measurement of air temperature, even for a perfectly ventilated and calibrated shipboard thermometer.

Spectroradiometers mounted on ships in the Tropics are of course subjected to the same heating as conventional thermometers, both directly by insolation and indirectly from the ship. However, provided the instrument is not heated beyond its operating range (50°C) the internal calibration reduces the temperature dependences of the measurement to insignificant levels. This requires the instrument to be well designed, built, and maintained. In particular the effects of stray radiation falling on the detectors must be small and well charac-

terized, so that accurate corrections can be made. This in turn requires additional temperature measurements to be made of the surfaces in and around the instrument that emit the stray radiation, and a sufficient understanding of the behavior of the instrument to allow these measurements to be used correctly.

Shipborne radiometers are not entirely immune from solar effects, and sunlight entering the aperture, either directly or by way of sun glint, can cause detectors to saturate and produce erroneous values. These are usually easy to identify and remove from the analyses. Other environmental effects that render the measurements inaccurate are precipitation, sea spray, and condensing or freezing fog on the scan mirror or entrance aperture window. These effects can be minimized by the careful use of baffles and when this fails, the consequences are generally easy to recognize and the data readily discarded.

Radiometric measurements of the air temperature will be contaminated by heat island effects if the volume of atmosphere sampled includes air heated by the ship. However, the positioning of instruments such as the M-AERI, whose primary objective is the measurement of the skin temperature of the ocean ahead of the bow wave of the ship, usually serves to reduce this likelihood. It is conceivable for situations to arise where the volume of sampled atmosphere does include heated air; these could be when the ship is drifting, on station, or making way slowly and the instrument is mounted on the lee side of the ship. There are indeed examples of this in the Nauru99 data from the R/V *Mirai*. Figure 9 shows an example of this where both radiometric and conventional air temperatures show a dependency on the relative wind direction. When the relative wind comes from the stern, the conventional air temperatures decrease and the radiometric ones increase. During this period the ship was making slow repeat circuits in the vicinity of the TOA mooring on the equator at 165°E. With the wind from the starboard stern sector, the volume of air sampled by the M-AERI, mounted on the foremast and viewing at about 30° from the bow to port, had passed over the heated ship, causing the air temperature to rise by nearly half a degree. It is interesting to note that the conventionally measured air temperature decreases by as much as a degree. This thermometer was mounted on the starboard side of the ship and therefore was much better ventilated under these conditions. In such cases, the radiometric data should be stringently examined for these effects, although it may not always be as straightforward for them to be recognized.

After removal of measurements taken when the relative wind was coming from between 135° and 180° relative to the bow, the daily amplitudes of the diurnal signal were calculated as the differences in the mean air temperatures in the hours centered at 1500 and 0800 local sun time (LST). These times generally marked the warmest and coolest values in each day. Only days where the sampling was sufficient to easily identify a clear diurnal signal are included in Table 5. The diurnal amplitudes in the radiometrically measured air temperatures are between 3 and 40 times smaller than in the conventionally measured data. Under these conditions, the average ratio of the amplitudes is 0.152.

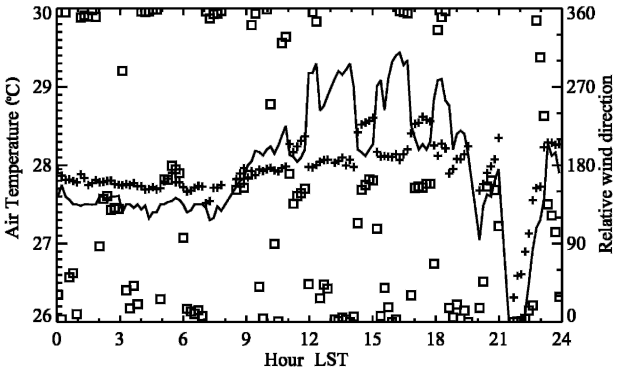

FIG. 9. Air temperatures measured on the R/V *Mirai* on 26 Jun 1999, by the conventional thermometer (solid line) and radiometrically by the M-AERI (plus signs). Also shown is the relative wind direction (squares). The increase in the radiometric temperature when the relative wind was between 135° and 180° of the bow is apparent between 1100 and 1200, 1400 and 1500, and 1700 and 1800 local solar time. Relative winds from this direction brought air into the M-AERI measurement volume that had passed over the ship. It is noteworthy that there is a reduction in the conventionally measured temperatures at the same times, indicating that the thermometer was better ventilated as it was on the upwind side of the ship. These effects are missing in the data taken at night (e.g., between 0200 and 0300, and 0500 and 0600 LST). The small bias in the air temperature differences measured at night is probably a calibration uncertainty in the conventional air temperature thermometer.

The small, but significant offsets found between the M-AERI and several conventional datasets, such as the *Mirai* data at night, and the comparisons with the fast-response thermometer on the *Radisson* have been attributed to uncertainties in the conventional measurements. This is based on our confidence in the absolute calibration of the M-AERI radiometry, not only through the use of accurate internal blackbody calibration targets (Minnett et al. 2001) and traceability to NIST standards (Rice et al. 2004), but also through comparisons with other radiometers (Barton et al. 2004). A direct comparison was possible during the Nauru99 cruise of the R/V *Mirai*, as the SISTeR (scanning infrared sea surface temperature radiometer) was mounted on the foremast platform along with the M-

TABLE 5. Amplitudes of the diurnal signal in air temperature in the equatorial Pacific. The measurements were taken from the Nauru99 cruise of the R/V *Mirai*, and those in which the relative wind was from the stern starboard sector have been discarded (see the text). Amplitudes were calculated as the differences in hourly averages centered at 1500 and 0800 (local sun time).

Date LST	Amplitude of diurnal signal in air temperature		
	Radiometric (K)	Conventional (K)	Ratio
10 Jun 1999	0.151	1.222	0.124
11 Jun 1999	0.270	1.230	0.219
14 Jun 1999	0.141	1.446	0.098
17 Jun 1999	0.301	1.712	0.176
18 Jun 1999	0.529	2.197	0.241
19 Jun 1999	0.261	1.827	0.143
20 Jun 1999	0.186	1.782	0.104
21 Jun 1999	0.383	2.476	0.155
22 Jun 1999	0.526	2.686	0.196
23 Jun 1999	0.440	1.962	0.224
24 Jun 1999	0.239	1.911	0.125
25 Jun 1999	0.300	1.953	0.154
26 Jun 1999	0.455	1.545	0.295
27 Jun 1999	0.134	1.297	0.103
28 Jun 1999	0.037	1.414	0.026
29 Jun 1999	0.244	1.700	0.144
30 Jun 1999	0.309	1.594	0.194
1 Jul 1999	0.174	1.511	0.115
2 Jul 1999	0.110	1.432	0.077
3 Jul 1999	0.194	1.535	0.126

AERI. The M-AERI viewed to port and the SISTeR to starboard. The SISTeR, described briefly by Barton et al. (2004), is a chopped self-calibrating filter radiometer that, like the M-AERI, includes two internal blackbody cavities of real-time calibration. Wavelength selection is done by a filter wheel that contains three narrowband filters centered at 3.7, 10.8, and 12.0 μm. During the R/V *Mirai* cruise, SISTeR radiances were sampled every 0.8 s with the 10.8-μm filter with a measurement cycle containing 128 samples, made up of 76 ocean samples at 48° from nadir, measurements of the sky emission for the reflection correction in the retrieval of skin sea surface temperatures, and measurements of the internal calibration targets. Over the period of the cruise, the mean and standard deviation of the differences in the M-AERI and SISTeR skin sea surface temperature retrievals was 0.003 ± 0.057 K ($n = 2414$). This is remarkable agreement given that the two instruments were looking at water on different sides of the bow of the ship (but both ahead of the bow wave), have differing operating principles, and have independent calibrations, each traceable to separate national standards (National Institute of Standards and Technology in the United States for M-AERI and the National Physical Laboratory in the United Kingdom for SISTeR). The M-AERI skin sea surface temperature retrievals are more uncertain than those of air temperature, which is simply the measurement of spectral radiance at selected wavenumbers, so this good agreement between skin sea surface temperature measurements in the field endorses our confidence in the M-AERI calibration and, consequently, on the accuracy of the air temperature measurement.

For most installations the M-AERI is mounted sufficiently high so that the contribution of emission from the sea surface to the sea-viewing measurement of atmospheric emission is negligible. On some ships, however, the instrument is mounted low above the waterline (<10 m elevation) and the error introduced into the air temperature retrieval by emission from the sea surface cannot be neglected. In such cases, a simple correction using the retrieved skin sea surface temperature and the assumption of a linear lapse rate appears to remove the contamination, insofar as it is revealed through a dependency on the air-surface temperature difference. The cruise data that were used to develop this correction are extreme in that they were taken from an ice-breaking research vessel in the Arctic, where very high values of air–sea temperature differences were experienced when airflow was off the ice. Differences in the surface skin sea surface temperature and the air temperature at an elevation of 6.5 m of up to 10 K were found. This is more than two orders of magnitude greater than normal circumstances over most of the world's oceans. Since the effect of the surface emission is related to this temperature difference, the residual errors in air temperature derived from the M-AERI, using the spectra measured at 55° view angles, is considered to be negligible.

Given that the radiometric measurement of air temperature is based on the natural thermal emission of CO_2 molecules in the atmosphere in the vicinity of the ship, unlike the conventional approach, it does not disturb the state of the atmosphere by the measurement procedure. The validation of the radiometric air temperatures is not straightforward, as they are inherently more accurate and more immune to the diurnal heat island and flow blockage effects than the conventional measurements, against which they are inevitably compared. To estimate the residual uncertainties, one has to rely on the excellent radiometric calibration of the M-AERI, which is well established by laboratory checks against NIST-traceable standards. These indicate residual uncertainties in the M-AERI spectral radiances, when expressed as temperatures, of ~0.02 K and less. While we cannot demonstrate this level of accuracy in the air temperature measurement in the field, it is indeed likely that this is being achieved. These residual uncertainties are below the specified

level of accuracy required for air temperature measurements at sea.

7. Conclusions

There is a wealth of information about the state of the atmosphere in the infrared emission spectra measured by a well-calibrated spectroradiometer. Included in this is the temperature of the air in the vicinity of the instrument. By a careful selection of a set of wavenumbers in the spectral region where the atmospheric emission is dominated by that from CO_2 molecules, measurement of air temperature within ~10 m of the sensor can be achieved, without compromising the accuracy of the real-time calibration procedure.

The radiometric measurements of marine air temperatures appear to be largely immune to the diurnal contamination that compromises conventional measurements, and which appears to be related to either direct solar heating of the thermometer or heat island effects of the ship. In a case study of measurements taken over a month in the equatorial Pacific Ocean, the amplitudes of the diurnal signal in the radiometrically measured air temperatures were found, on average, to be about a factor of 7 smaller than those in conventionally measured data.

It is very difficult to specify the accuracy of the radiometric air temperature measurement as, from what we know from laboratory and field measurements, this is much better than conventional measurements against which they are compared. The uncertainties in the spectral radiance measurements are very small indeed, especially when the air temperature is close to that of the ambient blackbody calibration target, which is nearly always the case, and it is then likely that the largest source of uncertainty is in the use of the average of the 55° up- and down-looking views or, in the case where M-AERI is mounted below ~10 m above the waterline, in the correction for the surface emission in the downward view. Both introduce additional uncertainties if the lapse rate is not linear. Even in these cases, it is very likely the residual uncertainties in the air temperature measurements are less than 0.1 K.

The M-AERI is a complex and costly instrument. So, while radiometric measurements of air temperature have significant advantages over conventional ones, it is not necessary that they be made with FTIR spectroradiometers. Well-calibrated filter radiometers could be designed to achieve comparable accuracy, as is the case for the measurement of skin sea surface temperatures (Barton et al. 2004). These could be deployed on research ships or selected voluntary observing ships to generate joint datasets with conventional thermometers to provide a basis for improved corrections to the existing databases of marine air temperatures (e.g., Kent et al. 1993).

Acknowledgments. The captains, officers, and crews of the ships that have hosted the M-AERI are acknowledged for their at-sea support. The air temperature measurements from the R/V *Mirai* were made available by Dr. R. M. Reynolds of Brookhaven National Laboratory, the SISTeR measurements from the *Mirai* by Dr. T. N. Nightingale of the Rutherford Appleton Laboratory in the United Kingdom, and the air temperatures from the Flux Mast on the NGCC *Pierre Radisson* by Dr. T. Papakyriakou of the University of Manitoba, Canada. Comments on an earlier draft by Dr. Elizabeth Kent of the Southampton Oceanography Centre, United Kingdom, have helped clarify the presentation. NASA funded the development of the M-AERI at the Space Science and Engineering Center, University of Wisconsin—Madison, through Contract NAS5-31361 to O. B. Brown, University of Miami. NASA also supported the fieldwork on the on the R/V *Mirai* and the NGCC *Pierre Radisson.* The NSF supported the cruise on the R/V *Tangaroa* (OCE 0327188).

REFERENCES

Anderson, S. P., and M. F. Baumgartner, 1998: Radiative heating errors in naturally ventilated air temperature measurements made from buoys. *J. Atmos. Oceanic Technol.,* **15,** 157–173.

Barton, I. J., P. J. Minnett, C. J. Donlon, S. J. Hook, A. T. Jessup, K. A. Maillet, and T. J. Nightingale, 2004: The Miami2001 infrared radiometer calibration and inter-comparison. Part II: Ship comparisons. *J. Atmos. Oceanic Technol.,* **21,** 268–283.

Berry, D. I., and E. C. Kent, 2005: The effect of instrument exposure on marine air temperatures: An assessment using VOSClim data. *Int. J. Climatol.,* in press.

——, ——, and P. K. Taylor, 2004: An analytical model of heating errors in marine air temperatures from ships. *J. Atmos. Oceanic Technol.,* **21,** 1198–1215.

Clough, S. A., and M. J. Iacono, 1995: Line-by-line calculations of atmospheric fluxes and cooling rates II: Application to carbon dioxide, ozone, methane, nitrous oxide, and the halocarbons. *J. Geophys. Res.,* **100,** 16 519–16 535.

Donlon, C. J., and I. S. Robinson, 1996: Observations of the oceanic thermal skin in the Atlantic Ocean. *J. Geophys. Res.,* **102,** 18 585–18 606.

——, P. J. Minnett, C. Gentemann, T. J. Nightingale, I. J. Barton, B. Ward, and J. Murray, 2002: Toward improved validation of satellite sea surface skin temperature measurements for climate research. *J. Climate,* **15,** 353–369.

Fortier, M., 2003: CASES Canadian Arctic Shelf Exchange Study. CASES 2002 Cruise Rep. and Preliminary Data Rep., Universite Laval, 73 pp. [Available online at http://www.cases.quebec-ocean.ulaval.ca/fieldwor.asp.]

Fowler, J. B., 1995: A third generation water bath based blackbody source. *J. Res. Natl. Inst. Stand. Technol.,* **100,** 591–599.

Goerss, J. S., and C. E. Duchon, 1980: Effect of ship heating on dry-bulb temperature measurements in GATE. *J. Phys. Oceanogr.,* **10,** 478–479.

HMSO, 1994: Notes for observing officers. *Met. Obs.,* **64,** 129–132.

Kannenberg, R., 1998: IR instrument comparison workshop at the Rosenstiel School of Marine and Atmospheric Science (RSMAS). *Earth Obs.,* **10,** 51–54.

Katsaros, K., W. T. Liu, J. A. Businger, and J. E. Tilman, 1977: Heat transport and thermal structure in the interfacial boundary layer measured in a open tank of water in turbulent free convection. *J. Fluid Mech.,* **83,** 311–335.

Kearns, E. J., J. A. Hanafin, R. H. Evans, P. J. Minnett, and O. B. Brown, 2000: An independent assessment of Pathfinder AVHRR sea surface temperature accuracy using the Marine-Atmosphere Emitted Radiance Interferometer (M-AERI). *Bull. Amer. Meteor. Soc.,* **81,** 1525–1536.

Kent, E. C., R. J. Tiddy, and P. K. Taylor, 1993: Correction of marine air temperature observations for solar radiation effects. *J. Atmos. Oceanic Technol.,* **10,** 900–906.

Minnett, P. J., 2002: The Accuracy of tropical sea-surface temperatures measured by radiometers on TRMM. *First TRMM Int. Sci. Conf.*, Honolulu, HI, NASA.

——, 2003: Radiometric measurements of the sea-surface skin temperature—The competing roles of the diurnal thermocline and the cool skin. *Int. J. Remote Sens.,* **24,** 5033–5047.

——, 2004: Diurnal signals in air-sea temperature signals—True or false? *Eos, Trans. Amer. Geophys. Union,* **84** (52), OS311-08.

——, R. O. Knuteson, F. A. Best, B. J. Osborne, J. A. Hanafin, and O. B. Brown, 2001: The Marine-Atmospheric Emitted Radiance Interferometer (M-AERI), a high-accuracy, sea-going infrared spectroradiometer. *J. Atmos. Oceanic Technol.,* **18,** 994–1013.

——, R. H. Evans, E. J. Kearns, and O. B. Brown, 2002: Sea-surface temperature measured by the Moderate Resolution Imaging Spectroradiometer (MODIS). *IEEE Int. Geoscience and Remote Sensing Symp.,* Toronto, ON, Canada, IEEE.

——, and Coauthors, 2003: Sea surface temperature measurements from the MODerate-resolution Imaging Spectroradiometer (MODIS) on AQUA. *Eos, Trans. Amer. Geophys. Union,* **84** (46), H22H-03.

Morris, A. L., D. B. Call, and R. B. McBeth, 1973: A small tethered balloon sounding system. *Bull. Amer. Meteor. Soc.,* **56,** 964–969.

Post, M. J., and Coauthors, 1997: The Combined Sensor Program: An air-sea science mission in the central and western Pacific Ocean. *Bull. Amer. Meteor. Soc.,* **78,** 2797–2815.

Ramage, C. S., 1984: Can shipboard measurements reveal secular changes in tropical air-sea heat flux? *J. Climate Appl. Meteor.,* **23,** 187–193.

Rayner, N. A., D. E. Parker, E. B. Horton, C. K. Folland, L. V. Alexander, D. P. Rowell, E. C. Kent, and A. Kaplan, 2003: Global analyses of SST, sea ice and night marine air temperature since the late 19th century. *J. Geophys. Res.,* **108,** 4407, doi:10.1029/2002JD002670.

Revercomb, H. E., H. Buijs, H. B. Howell, D. D. LaPorte, W. L. Smith, and L. A. Sromovsky, 1988: Radiometric calibration of IR Fourier transform spectrometers: Solution to a problem with the High Resolution Interferometer Sounder. *Appl. Opt.,* **27,** 3210–3218.

Rice, J. P., and B. C. Johnson, 1998: The NIST EOS Thermal-Infrared Transfer Radiometer. *Metrologia,* **35,** 505–509.

——, and Coauthors, 2004: The Miami2001 infrared radiometer calibration and intercomparison. Part I: Laboratory characterization of blackbody targets. *J. Atmos. Oceanic Technol.,* **21,** 258–267.

Saunders, P. M., 1967: The temperature at the ocean-air interface. *J. Atmos. Sci.,* **24,** 269–274.

Shaw, J. A., D. Cimini, E. R. Westwater, Y. Han, H. M. Zorn, and J. H. Churnside, 2001: Scanning infrared radiometer for measuring air-sea temperature difference. *Appl. Opt.,* **40,** 4807–4815.

Smith, W. L., and Coauthors, 1996: Observations of the infrared radiative properties of the ocean—Implications for the measurement of sea surface temperature via satellite remote sensing. *Bull. Amer. Meteor. Soc.,* **77,** 41–51.

Williams, E., E. Prager, and D. Wilson, 2002: Research combines with public outreach on a cruise ship. *Eos, Trans. Amer. Geophys. Union,* **83,** 590–596.

Woodcock, A. H., and H. Stommel, 1947: Temperatures observed near the surface of a fresh water pond at night. *J. Meteor.,* **4,** 102–103.

Yelland, M. J., B. I. Moat, P. K. Taylor, R. W. Pascal, J. Hutchings, and V. C. Cornell, 1998: Wind stress measurements from the open ocean corrected for airflow distortion by the ship. *J. Phys. Oceanogr.,* **28,** 1511–1526.